General and Comparative Endocrinology 374 (2025) 114825

Contents lists available at ScienceDirect

General and Comparative Endocrinology

journal homepage: www.elsevier.com/locate/ygcen

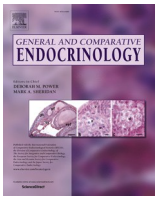

Stress signaling via glucocorticoid receptor disrupts ovarian development in Japanese eel (*Anguilla japonica*) through HPI-HPG axis crosstalk

Xuanhan Zhang [a], Chenpeng Zuo [a], Jiaqi Liu [a], Xiao Jing [a], Ziyi Zhao [a], Jing Yang [a], Zhijun Wang [b], Xin Qi [a,*]

[a] Key Laboratory of Mariculture, Ministry of Education (KLMME), Ocean University of China, Qingdao 266003, China
[b] Administration Department, Weihai Taifeng Seawater Seedling Co., LTD, Weihai, China

ARTICLE INFO

Keywords:
Japanese eel
Glucocorticoid receptor
Stress
Ovarian development
HPG axis

ABSTRACT

Gonadal development is closely linked to cortisol levels, a major stress response indicator, which is mediated by the glucocorticoid receptor (GR) in teleost fish. Stress activates the HPI axis (hypothalamic-pituitary-adrenocortical axis), triggering cortisol release, which subsequently affects the reproductive system. Therefore, GR is considered a mediator in elucidating the relationship between stress and gonadal development. In this study, we cloned and analyzed the *gr1* and *gr2* genes of the Japanese eel (*Anguilla japonica*). The phylogenetic tree of GR revealed that *gr1* and *gr2* exhibit a unique evolutionary distribution in teleost fish. Quantitative real-time PCR results indicated that *gr1* and *gr2* were primarily expressed in the ovary and brain. To investigate whether glucocorticoids mediate their inhibitory effects through GR, we performed *in vivo* DXMS injection experiments. The results indicated that DXMS stimulation significantly altered the expression of key genes in the HPG axis (hypothalamic-pituitary–gonadal axis) of the Japanese eel, particularly those related to ovarian development. Additionally, *in vitro* experiments with isolated brain, pituitary, and gonadal cells revealed that DXMS treatment significantly suppressed the expression of several reproduction-related genes, and the GR antagonist RU486 partially reversed this suppression. This study reveals the mechanisms through which glucocorticoids regulate ovarian development in the Japanese eel via GR and HPI-HPG axis interactions. These findings offer new insights into the role of stress in fish reproduction and provide a theoretical basis for optimizing artificial reproduction techniques in the Japanese eel.

1. Introduction

Glucocorticoids (GCs) are stress-responsive steroids, functioning as the final humoral effectors of the hypothalamic–pituitary–adrenal (HPA) axis (Breen and Karsch, 2006). In teleosts, the homologous pathway is the hypothalamic-pituitary-interrenal (HPI) axis (Whirledge and Cidlowski, 2013). The adrenal (or interrenal) cortex secretes cortisol and corticosterone, which are the primary GCs in vertebrates (Suarez-Bregua et al., 2018; Vazzana et al., 2010). These hormones regulate inflammation, metabolic processes, reproduction and the systemic stress response (Charmandari et al., 2005). In mammals and most teleost fish, cortisol serves as the primary endogenous GC (Arterbery et al., 2011; Li et al., 2012). In teleosts, activation of the HPI axis during stress has been shown to lead to a rapid elevation of circulating cortisol levels (Liu et al., 2016). Cortisol exerts its effects through two nuclear receptors: the glucocorticoid receptor (GR) and the mineralocorticoid receptor (MR), and GR has been identified as the principal mediator of cortisol's biological actions in teleosts (Reyes-López et al., 2018). Moreover, the GR also acts as an essential feedback regulator of the HPI axis (Bury et al., 2003; Liu et al., 2016).

GR, also known as NR3C1 (nuclear receptor subfamily 3, group C, member 1), is a ligand-activated nuclear receptor that regulates gene transcription and thereby cellular physiology (Dinarello et al., 2020; Weikum et al., 2018). Around 320–350 million years ago, teleosts experienced a third-round whole-genome duplication (T-WGD), resulting in most species retaining two GR paralogues (*gr1* and *gr2*) but only a single MR (Arterbery et al., 2011; Bury, 2017). GR has a modular architecture: an N-terminal structural domain (NTD), a DNA-binding structural domain (DBD), a hinge region (HR structural domain), and a ligand-binding structural domain (LBD); the DBD (two zinc fingers) recognizes GREs, and the LBD binds hormone and contains the AF-2 for ligand-dependent activation (Kumar and Thompson, 2005; Liu et al., 2019; Weikum et al., 2018). Functionally, GR integrates stress and metabolic regulation and can modulate reproduction, including ovarian

* Corresponding author.

https://doi.org/10.1016/j.ygcen.2025.114825
Received 28 July 2025; Received in revised form 16 September 2025; Accepted 1 October 2025
Available online 10 October 2025

gene expression and gonadal development (Bourke et al., 2012; Fernandino et al., 2012; Kirby et al., 2009).

The Japanese eel (*Anguilla japonica*) belongs to the Anguillidae family and displays a unique life cycle and reproductive strategy (Kagawa et al., 1998). Despite substantial progress in the artificial propagation of Japanese eel over the years, issues such as delayed ovarian development and inadequate oocyte maturation still persist. Environmental factors and hormonal regulation are known to restrict ovarian development (Lai et al., 2022); however, the impact of stress on artificial reproduction in the Japanese eels remains poorly understood. During artificial maturation, repeated handling and hormone injections may expose eels to chronic stress, potentially activating the HPI axis and elevating cortisol levels (Blanes-García et al., 2022). In Japanese eel, cortisol is synthesized via the interrenal tissue and regulates stress physiology (Jiang et al., 1998). Cortisol, acting through GRs, is expressed in reproductive tissues and influences gene transcription relevant to reproduction (Tokuda et al., 1999). Cross-talk between the HPI and hypothalamic-pituitary–gonadal (HPG) axes has been well documented in teleosts, where elevated cortisol disrupts reproductive function by suppressing gonadotropin-releasing hormone (GnRH) and gonadotropin signaling and impairing steroidogenesis (Milla et al., 2009). More recently, cortisol was shown to directly inhibit GnRH expression in fish, supporting its broader inhibitory role in reproductive endocrine control (Murugananthkumar and Sudhakumari, 2022). In eels, cortisol and corticotropin-releasing hormone (CRH) signaling can modulate GnRH neurons in the brain (Amano et al., 2014). Moreover, in the Japanese eel, gonadotropin receptor (GthR) expression is tightly regulated during oogenesis and is susceptible to hormonal modulation (Kazeto et al., 2012). In addition to gonadotropins, kisspeptin has emerged as a key upstream regulator of GnRH neurons, linking environmental cues to puberty and gonadal maturation, and its interaction with stress pathways suggests a potential target of GC action (Gopurappilly et al., 2012; Somoza et al., 2020; Zmora et al., 2012). At the pituitary level, gonadotropins (FSH and LH) act as central mediators of ovarian function by regulating steroidogenic enzymes and receptor expression (Weltzien et al., 2004). Within the ovary, local growth factors such as *igf3*, *bmp15*, and *gdf9* are essential for oocyte development, steroidogenesis, and follicle-granulosa cell communication (Knight and Glister, 2006; Reinecke, 2010). Stress-induced GC elevation may therefore disrupt reproduction not only by suppressing GnRH and gonadotropin signaling, but also through modulation of kisspeptin and intra-ovarian growth factor pathways, ultimately inhibiting ovarian development and oocyte maturation. Taken together, current evidence suggests that cortisol, acting through GR activation, may modulate reproductive hormone signaling in teleosts. In Japanese eel, such GR-mediated GC action may be a key factor limiting successful artificial reproduction.

In this study, we aimed to clarify the role of GR signaling in reproductive regulation of the Japanese eel under chronic stress. Our objectives were to characterize the domains and evolutionary relationships of *gr1* and *gr2*, examine their tissue-specific expression, and assess how GR activation influences the HPG axis. To simulate chronic stress, we used dexamethasone (DXMS), a synthetic GC analog with high selectivity for GR agonist activity that mimics cortisol signaling (Lutton and Callard, 2008; Pierce et al., 2010). To test the specificity of GC action, we applied mifepristone (RU486), a potent GR antagonist that blocks GR-mediated transcription (Lee et al., 2009). Together, these approaches allowed us to evaluate whether GR-mediated signaling directly contributes to reproductive suppression in the Japanese eel.

2. Materials and methods

Ethics statement

All animal experiments were approved by the Institutional Animal Care and Use Committee of Ocean University of China (Permit Number: 20141201). The animal care protocol was also approved by the Committee on the Ethics of Animal Experiments. Prior to euthanasia, experimental fish were anesthetized with 100 ng/ml ethyl 3-aminobenzoate methanesulfonic acid (MS222), and efforts were made to minimize animal suffering. The field studies did not involve endangered or protected species.

2.1. Fish and sampling

The female Japanese eels used in this study (approximately 4 years old, ~1.5 kg body weight) were purchased from Weihai, Shandong Province, in mid-September and temporarily housed in the seawater recirculation system at Qingdao Agricultural University. After 12 weeks of injection treatment, the eels were euthanized and tissue samples were collected. Eels for *in vitro* culture were purchased from the Qingdao Aquatic Market and sampled following temporary rearing in the laboratory.

2.2. Total RNA extraction and reverse transcription

Total RNA was extracted from brain, ovarian and pituitary tissues using TRIzol reagent (Vazyme, China) according to the manufacturer's instructions. RNA quantity and purity were assessed by a Biodropsis BD-1000 nucleic acid analyzer (OSTC, China) and by electrophoresis using a 1 % agarose gel. cDNA was prepared using the HiScript® III SuperMix (+gDNA wiper) kit (Vazyme, China) according to the manufacturer's instructions.

2.3. Molecular cloning and sequencing of gr1, gr2

The *gr1* and *gr2* Open Reading Frame (ORF) were cloned and validated using data from the Japanese eel genome (GCA_025169545.1). Primers used in this study are listed in Table 1. Ovarian cDNA was used as the template for cloning. The PCR product was purified, inserted into the pCE2 TA/Blunt-Zero vector (Vazyme, China) and sequenced.

2.4. Multiple alignments, phylogenetic tree construction and homologous modeling

Amino acid sequences of GRs from multiple species were aligned using ClustalX 2.1 and visualized with ESPript 3.0 (https://espript.ibcp.fr/ESPript/cgi-bin/ESPript.cgi). A phylogenetic tree was constructed based on the multiple sequence alignment using the neighbor-joining method in MEGA X. Bootstrap values from 1000 replicates are shown at the branch nodes to indicate the reliability of the inferred clades. The tertiary structures of the GR DBD and LBD were predicted by homology modeling using SWISS-MODEL (https://swissmodel.expasy.org/), and the resulting structures were visualized using PyMOL 2.4.

2.5. Quantitative real-time PCR

Quantitative real-time PCR (qPCR) was performed to quantify the expression levels of *gr1*, *gr2*, and genes involved in the HPG axis in the Japanese eel tissues. All primers used in this study are listed in Table 1. qPCR reactions were performed using the ChamQ™ SYBR & Color qPCR Master Mix (High Rox Premixed) kit (Vazyme, China) according to the manufacturer's instructions. The qPCR thermal cycling conditions were as follows: initial denaturation at 95 °C for 30 s; followed by 40 cycles of 95 °C for 10 s and 60 °C for 30 s. The melting curve analysis was performed at 95 °C for 15 s, 60 °C for 60 s, and 95 °C for 15 s. Threshold cycle (Ct) values were obtained for each sample. *18S* rRNA (GenBank accession number: AB038053.1) was used as the internal reference gene. Relative mRNA expression levels were calculated using the $2^{-\Delta\Delta C_T}$ method based on three biological replicates. All qPCR reactions were performed in triplicate to ensure reproducibility.

Table 1
The primers used for clone, ISH and qPCR.

Primer	Sequence (5′-3′)	Primer Usage
gr1-F	GGGAGCCTTTCAGAGTGGTG	Gene clone
gr1-R	AGGCATCTTGTCGCACTGTA	
gr2-F	TACTGTCCAGGGAGACCAAGC	Gene clone
gr2-R	TTCGCCCTTCCCTTCATCCTC	
18S-F	AAAGCGGTTCTCAGTGTCGT	RT-qPCR
18S-R	CTCAAAGGCACGCGAGAAAG	
gr1-qF	AGCAAAGCAAACCAGTTGCC	RT-qPCR
gr1-qR	CTGACGGCACAATCCGAAAC	
gr2-qF	CAGGTGGCGTTTGAGGAGAT	RT-qPCR
gr2-qR	TCTCCACCAGCATCTCAGGA	
gr1-IF	CGCATTTAGGTGACACTATAGAAGCGATGGGCAGCAATAACCCTCA CCGTAATACGACTCACTATAGGGAGACAGAAACAGCTGTACGAATGTG	ISH
gr1-IR	CGCATTTAGGTGACACTATAGAAGCGGAGGTCATCAGTGTCCAGCC	
gr2-IF	CCGTAATACGACTCACTATAGGGAGACACAGGTAAGTGGTCTCCGCTG	ISH
gr2-IR	ACGCTTTCAGTGCCGACATA	
cgnrh-qF	CCACAACAGTGTGCGAGAAC	RT-qPCR
cgnrh-qR	ACAGGACACGCTGCAAGATA	
mgnrh-qF	TGTCAGCCAGATTTGCCAGTA	RT-qPCR
mgnrh-qR	CCTTCACAGGAGGTCGTGG	
kisspeptin1-qF	CGTAGCGTAGACCGAAAGAGT	RT-qPCR
kisspeptin1-qR	CGGCCAACTCCATTGAACAC	
cox2-qF	TCCACTGCGTCAATGTCTCC	RT-qPCR
cox2-qR	CTCCGATCATGCCAGTCCAG	
tac3-qF	TGAACTCCTCCGACCCATCA	RT-qPCR
tac3-qR	CCAACAACGAAATGGCACGA	
gthα-qF	GGAGAAACAGCAACCAACGC	RT-qPCR
gthα-qR	GCGGCAAGGGATAGATGCTT	
fshβ-qF	GCCATTAACCGTGCAAGACA	RT-qPCR
fshβ-qR	TTACTGCTGCCTTGTGAGCC	
lhβ-qF	TAGCTTGGGTCCTTGGTGATG	RT-qPCR
lhβ-qR	CCGGGTGATTAAGGCAGAGG	
gnrhr-qF	ACAACGTAGAGCGTGACGAA	RT-qPCR
gnrhr-qR	GCTCGGATGAAGACGCTGAA	
gnrhr1α-qF	TGAGGTTGCCGAAGACGAAG	RT-qPCR
gnrhr1α-qR	GGTGTCCTTTGTGGTCTGCT	
gnrhr1β-qF	GTCACAGCAGGTGTTGAGGT	RT-qPCR
gnrhr1β-qR	TGGAGTTATGTTCCACCGGC	
gnrhr2-qF	ATCAGGATTCTCACGGTCGC	RT-qPCR
gnrhr2-qR	AACTACTCCTCCTGCGACCC	
gnrhr4-qF	GAGATCACGCACAGGACGAA	RT-qPCR
gnrhr4-qR	CAGGGTATGGAAGGACCACG	
cyp11a1-qF	GGCCAGCTCATACAGAGTCC	RT-qPCR
cyp11a1-qR	TTTGCAGGGAGACCGAGAAC	
cyp17a1-qF	CACTAGGGCCTGACACATGG	RT-qPCR
cyp17a1-qR	CCTGCGTTGGGAAACACATC	
cyp19a1a-qF	TTGCGACAGGTTGTTGGTCT	RT-qPCR
cyp19a1a-qR	GAACCTGGTGGGAAACGGAT	
lhr-qF	TTCGAAGGCTTCATCGTGGA	RT-qPCR
lhr-qR	ATGCCCACCGTCATCCCAAA	
fshr-qF	TCGACCAGGTTTGATAGGTTCG	RT-qPCR
fshr-qR	TGGGAGAGAGGATCTGCCG	
3β-hsd-qF	ATGCTTGAAGGGACTGGACAA	RT-qPCR
3β-hsd-qR	AACTTTCAAACTGTGCGCCG	
star-qF	GCCTGCTCAGCTCATGGTTA	RT-qPCR
star-qR	TACTGCGCCAAACCACTCC	
igf3-qF	CTTCCAGTCTCTGTGCTGTGT	RT-qPCR
igf3-qR	ATGATGGCACCTCAAAGCGT	
ddit4-qF	CACTCCGGCTGCAACTATCA	RT-qPCR
ddit4-qR	CAAATGTAACCCGGCCAACC	
klf9-qF	TACACTTTGCCACAACCGGA	RT-qPCR
klf9-qR	GGGTTTTCGTTGGCTTTCCC	
gdf9-qF	CAGGGATTAGTTTCGGGGCA	RT-qPCR
gdf9-qR	AAAGCGGTTCTCAGTGTCGT	
bmp15-qF	CTCAAAGGCACGCGAGAAAG	RT-qPCR
bmp15-qR	CACTCCACCGTCATCAACCA	
inhba-qF	TGACGATCTTGTGCTCCTCG	RT-qPCR
inhba-qR	TGGACAACCAGAAGAATCGG	
inhbb-qF	GGGTGATGTTCGGTCTTTCT	RT-qPCR
inhbb-qR		

2.6. Preparation of DIG-labeled riboprobes and in situ hybridization (ISH)

Primers with T7 or SP6 RNA polymerase recognition sites (Table 1) were designed for PCR amplification of DNA templates for RNA probes. Antisense and sense RNA probes for *gr1* and *gr2* were synthesized *in vitro* using the DIG RNA Labeling Kit (SP6/T7) (Roche, Switzerland). Ovarian, brain, and pituitary tissues from Japanese eels were fixed in 4 % paraformaldehyde in PBS (pH 7.4) for 4–6 h, then embedded in paraffin and sectioned at 7 μm thickness. Tissue sections were

deparaffinized, rehydrated, and treated with RNase-free solutions: 0.2 M HCl (8 min [min]), PBS (2 × 5 min), 10 μg/mL proteinase K in PBS (37 °C, 5 min), PBS (5 min), 0.1 M triethanolamine-HCl (pH 8.0), 0.25 % acetic acid (10–15 min), and 2 × SSC (5 min). Sections were pre-incubated at 55 °C for 1 h in hybridization buffer (50 % deionized formamide, 5 × SSC, 5 × Denhardt's solution, 1 mg/mL yeast tRNA, 10 % dextran sulfate) without probe. RNA probes (1.5 μg/mL) were diluted in hybridization buffer, applied to the slides, and incubated at 55 °C in a humidified chamber. After overnight hybridization (12–16 h), slides were washed in prewarmed 2 × SSC, 1 × SSC, 0.2 × SSC, and 0.1 × SSC at 55 °C for 15–30 min per step. DIG-labeled probes were detected using anti-DIG Fab fragments (1:400 dilution) and NBT/BCIP substrate (Roche, Switzerland). Sections were dehydrated, mounted, and examined under a light microscope.

2.7. Radioimmunoassay of serum cortisol

Prior to the injection experiment, ten Japanese eels were allocated into two groups. Five eels in the control group were kept undisturbed in the tank for 12 weeks without any injection treatment, in order to avoid additional handling stress and to serve as a true baseline. The other five eels were subjected to weekly handling and intraperitoneal saline injections for 12 weeks to simulate the process of artificially induced ovarian development. In this group, fish were gently netted from the tank each week before injection. At the end of the 12-week period, blood samples were collected from all ten eels; serum was not collected after each injection to prevent repeated handling stress. Serum cortisol levels were measured using a Cortisol Iodine-125 [^{125}I] Radioimmunoassay Kit (Nanjing Jiancheng, China), with a sensitivity of 0.15 ng/mL and a detection range of 10–500 ng/mL, suitable for accurate measurement in fish.

2.8. Haematoxylin-eosin (H&E) staining

Ovarian tissues were fixed in 4 % paraformaldehyde, embedded, and sectioned into 7-μm slices. The sections were stained with hematoxylin and eosin and subsequently observed and photographed under an Olympus bright-field light microscope (Olympus, Tokyo, Japan).

2.9. In vivo GC treatment

Japanese eels were maintained in a recirculating water system for three weeks, followed by weekly hormone injections for 12 weeks. The control group received human chorionic gonadotropin (hCG, 300 IU/kg; National Standard Hormone Factory, NSHF, China) and luteinizing hormone-releasing hormone analogue-2 (LHRH-A2, 15 μg/kg; NSHF, China), which are widely used for inducing artificial maturation in eels and therefore served as a physiologically relevant baseline treatment. The experimental group was treated with DXMS (10 μg/kg, Yuanye, China) in combination with the same hormones, using saline as the injection vehicle. Each group consisted of seven eels. After the injection period, fishes were euthanized, and ovarian, brain, and pituitary tissues were collected for molecular and histological analyses.

2.10. In vitro GC and RU486 treatment

DXMS (10^{-6} mol/L) and RU486 (10 ng/mL, Aladdin, Shanghai) were dissolved in anhydrous ethanol to prepare stock solutions. Ovarian tissues from Japanese eels were washed with antibiotics (penicillin and streptomycin) and digested in Trypsin-EDTA (Servicebio, China) for 5–10 min at room temperature. Digestion was stopped by adding an equal volume of L-15 complete medium (Biological Industries, Israel) containing antibiotics and 10 % fetal calf serum. The suspension was filtered (40 μm), centrifuged, and resuspended in L-15 medium. Cells were seeded into 12-well plates and incubated at 25 °C for 24 h in a CO_2-free incubator. After 2 h of serum starvation, cells were divided into three groups and treated in quadruplicate. The control group received 0.1 % ethanol vehicle. A second group was treated with diluted DXMS (10^{-6} mol/L) for 6 h. In the third group, cells were pretreated with RU486 (10 ng/mL) for 3 h followed by DXMS (10^{-6} mol/L) for 3 h. At the end of stimulation, Trizol was added for RNA extraction and qPCR. Brain and pituitary tissues from 15 eels were also washed with antibiotics. Pituitary cells were treated as above. Brain cells were cultured using the tissue block method: tissues were minced, transferred to 24-well plates, allowed to settle for 30 min, and cultured in complete medium for 2 h before applying the same stimulation protocol.

2.11. Statistical analysis

All data are presented as the mean ± standard error of the mean (SEM). Graphs were generated using GraphPad Prism 9 (GraphPad Software, USA). Data of serum cortisol levels and gene expression of *in vivo* treatment were analyzed using Student's *t*-test with GraphPad Prism 9. The data of *in vitro* treatment were subjected to one-way ANOVA followed by Tukey's multiple comparison test. A value of $P < 0.05$ was considered statistically significant.

3. Results

3.1. Molecular cloning and sequence analysis

In total, two *gr* genes (*gr1* and *gr2*) were identified in the Japanese eel. The ORF of *gr1* is 2085 base pairs (bp) (GenBank accession number: PV927314), encoding a precursor protein of 694 amino acids (aa). The ORF of *gr2* is 2811 bp (GenBank accession number: PV927315), encoding a protein of 936 aa. Based on the amino acid alignment, it was determined that vertebrate GR proteins have four modular structural domains: NTD, DBD, HR and LBD (Fig. 1A). The overall amino acid identity between the two GRs in the Japanese eel was 53.76 %, with high sequence identities in the DBD (88.03 %) and LBD (83.07 %) regions, and lower identities in the NTD (36.61 %) and HR (40.44 %) regions (Fig. 1B). Most teleosts had two copies of GR genes, while basal ray-finned fishes, ray-finned fishes and tetrapods had only one copy.

The DBD of vertebrate GRs contain two highly conserved C4-type zinc fingers (Fig. 1**C, D**), each comprising four cysteine residues that coordinate with zinc ions (Zn^{2+}). The LBD homology model reveals a typical and highly conserved α-helix fold, and molecular docking analysis indicates that its internal cavity can accommodate cortisol molecules (Fig. 1**E, F**).

Phylogenetic analysis revealed that the two GR genes (GR1 and GR2) of Japanese eel clustered within the classical GR1 and GR2 clades of teleosts, respectively, while each formed a distinct sub-branch within its corresponding lineage, indicating species-specific divergence (Fig. 1G). The clustering pattern indicates that both isoforms are retained in the Japanese eel and share high sequence similarity with GR isoforms of other teleosts. Specifically, GR1 of Japanese eel clustered into a well-supported sister clade with GR1 of European eel (*Anguilla anguilla*), and this clade further grouped with GR1 sequences from other teleost species to form a major GR1 branch, exhibiting high conservatism and lineage specificity. Similarly, GR2 of the Japanese eel clustered with GR2 of the European eel and was grouped into the major GR2 branch, further supporting that the two *gr* gene subtypes, *gr1* and *gr2*, are highly conserved within the *Anguilla* genus (Fig. 1G). Additionally, the separate clustering of *gr1* and *gr2* in the Japanese eel supports their origin from the T-WGD event and their retention following species divergence. The phylogenetic model not only confirms the presence and taxonomic positioning of GR1 and GR2 in the Japanese eel, but also offers a robust evolutionary basis for further studies on the functional divergence between these two GRs isoforms in regulating the HPI and HPG axes and their role in stress-reproduction crosstalk.

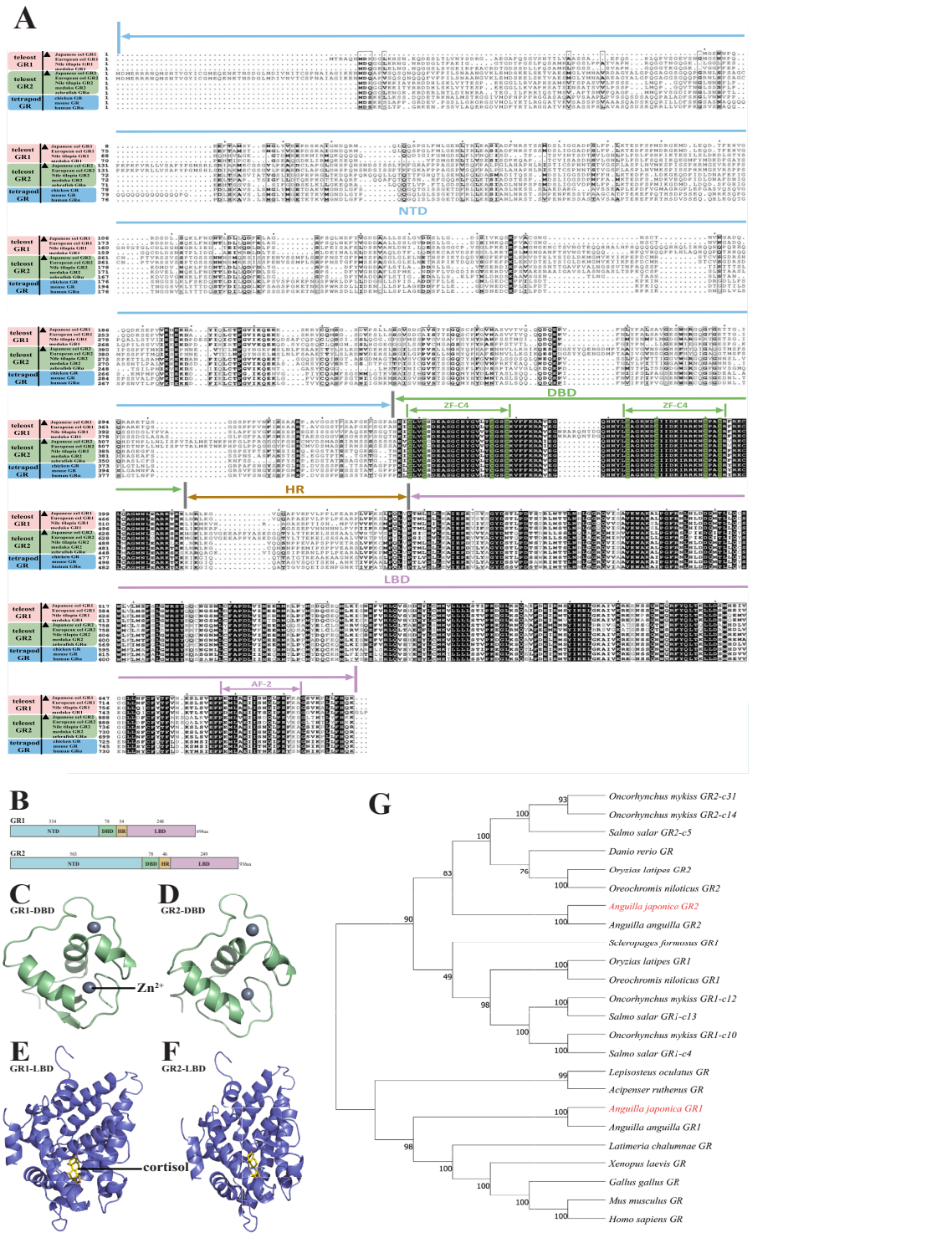

Fig. 1. Comparative analysis of vertebrate GRs: Sequence Alignment (A), Structural Characteristics (B), and Phylogenetic Relationships (C). A: AF-2: activation function domain-2; ZF-C4: C4-type zinc finger–the electron donors for Zn^{2+} (cysteines) are painted in green. The GenBank accession numbers of GR sequences used in this study are as follows: *Homo sapiens* GRα (NP000167.1); *Mus musculus* GR (NP001348138.1); *Gallus gallus* GR (XP015149519.1); *Danio rerio* GRα (NP001018547.2); *Oryzias latipes* GR1 (NP001292330.1), GR2 (NP001156605.1); *Oreochromis niloticus* GR1 (XP003446987.1), GR2 (XP013127157.1). *Anguilla Anguilla* GR1 (XP035264737.1), GR2 (XP035281384.1). B-F: B: Linear structures. C, D: Predicted 3D structures of GR DBD using tetrapod GR DBD as a template (Protein Data Bank ID code: 1glu.1). E, F: Predicted 3D structures of GR LBD using tetrapod GR LBD as a template (Protein Data Bank ID code: 4p6x.5.A). G: The GenBank accession numbers for the sequences are *Xenopus laevis* GR (NP001081531.1); *Latimeria chalumnae* GR (XP005996163.1); *Lepisosteus oculatus* GR (XP015204944.1); *Acipenser ruthenus* GR (AFK14015.1); *Scleropages formosus* GR1 (XP018607685.1), GR2 (XP018611937.1); *Oncorhynchus mykiss* GR1-c12 (XP036793674.1), GR1-c10 (NP001118202.1), GR2-c31 (XP036826413.1), GR2-c14 (NP001117954.1); *Salmo salar* GR1-c13 (XP013992257.1), GR1c4 (XP014053534.1), GR2-c5 (XP014054152.1). *Anguilla Anguilla* GR (XP035264737.1), GR2 (XP035281384.1).

3.2. Tissue distribution of gr1 and gr2 mRNA in Japanese eel

mRNA tissue distribution analysis indicated that *gr1* and *gr2* genes are expressed in a tissue-specific manner across various tissues of the Japanese eel (Fig. 2**A, B**). Among them, the ovary exhibited the highest expression levels, particularly for *gr2*, which was highly concentrated, indicating strong tissue specificity. In contrast, *gr1* showed broader expression, with detectable levels in the brain and muscle.

In the ovaries, *gr* transcripts were predominantly localized in oocytes (Fig. 2**C1-C4**). In the brain, *gr1* and *gr2* mRNA was mainly localized in hypothalamic neuronal nuclei, such as nucleus preopticus (NPO), nucleus preopticus parvocellularis (NPP), and nucleus diffusus lobi (NDL) (Fig. 2**D1-D16**), while in the pituitary, *gr* transcripts were concentrated in the rostral pars distalis (RPD), proximal pars distalis (PPD), and neurohypophysis (NH) regions (Fig. 2**E1-E12**) (Mukuda and Ando, 2003).

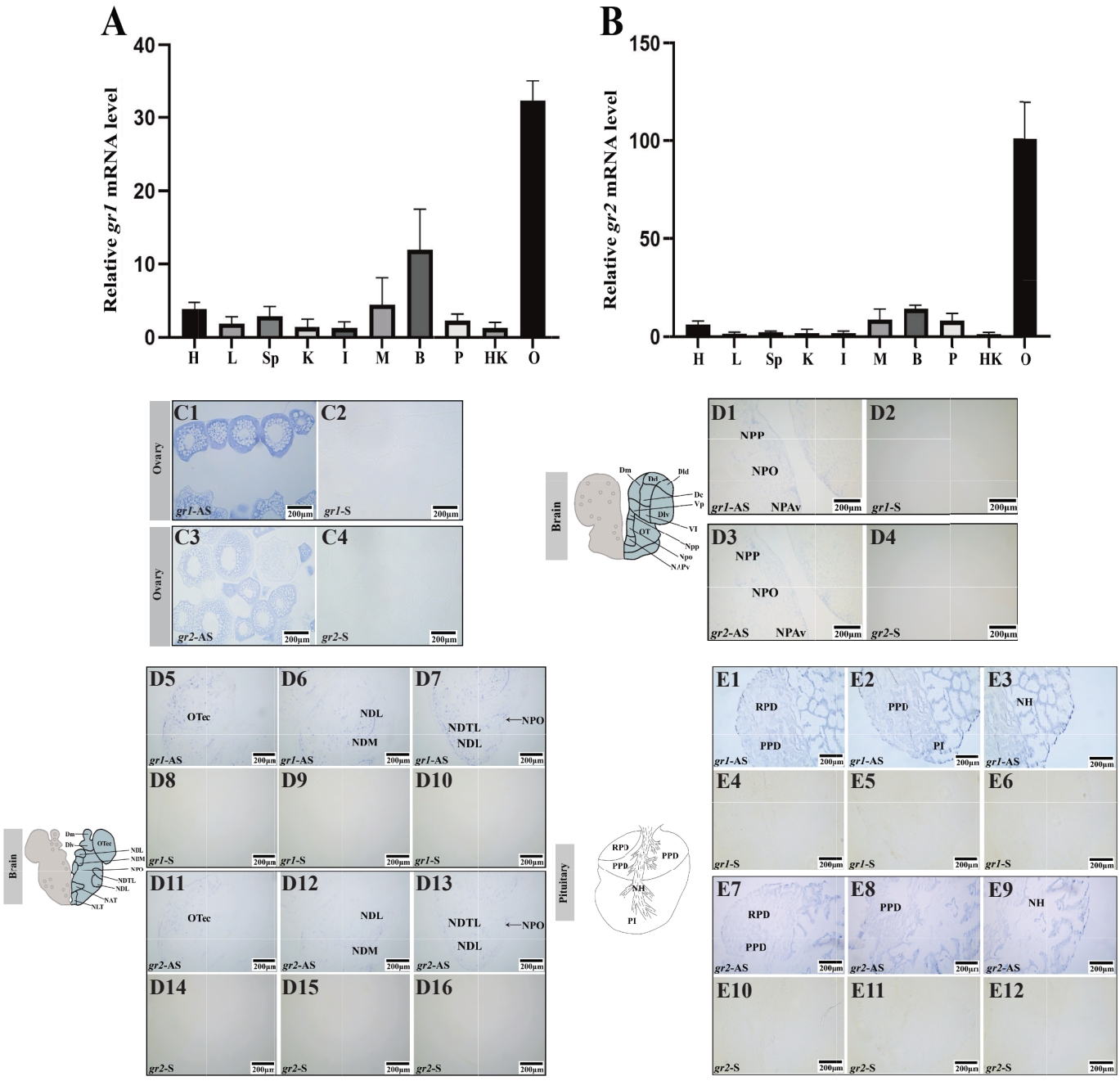

Fig. 2. mRNA tissue distribution of *gr1* (A), *gr2* (B) and *in situ* hybridization of *gr1* and *gr2* in the ovary (C), brain (D), and pituitary (E) of Japanese eel. C1-C4: ovary; D1-D16: brain; E1-E12: pituitary. O: ovary at the vitellogenesis stage; T: mature testis; HK: head kidney; K: kidney; B: brain; P: pituitary; H: heart; L: liver; Sp: spleen; St: stomach; I: intestine; G: gill; Sk: skin; WM: white muscle. Bars with different letters indicate significant differences ($P < 0.05$). AS: tissue section treated with antisense probes; S: section treated with sense probes as a negative control.

3.3. Effects of stimulatory treatment on serum GCs and gonadal development in Japanese eel

Serum cortisol concentration increased significantly at the end of the 12-week injection cycle compared with the baseline level (Fig. 3A). The observed increase indicates a marked stress response during artificially induced ovarian development, accompanied by activation of the HPI axis and elevated GC secretion after 12 weeks of weekly saline injections.

In the experiment of artificially induced ovarian development, body coloration was used only as a rough external indicator of developmental stage; however, despite showing similar coloration, ovarian development differed among groups. In the DXMS-treated group, ovaries appeared smaller, showed reduced vascularization, and exhibited a more compact tissue structure, suggesting impaired development. H&E-stained sections further confirmed these histological findings. In the control group, oocytes showed normal development with well-defined cortical follicles and a large cytoplasmic area. By comparison, oocytes from the DXMS-treated group remained at an earlier developmental stage, exhibited a smaller cytoplasmic area, and displayed denser nuclei, indicating suppressed follicular development (Fig. 3B).

3.4. Effects of DXMS injection on the expression of key genes in the HPG axis

Following DXMS injection, several neuro-reproductive pathway genes were significantly downregulated in brain tissue, including chicken-type gonadotropin-releasing hormone (*cgnrh*), mammalian-type gonadotropin-releasing hormone (*mghrh*), and cyclooxygenase-2 (*cox2*) (Fig. 4A). Similarly, neurokinin B (*tac3*) expression was reduced (Fig. 4A), whereas *kisspeptin1* showed no significant difference between control and DXMS-treated groups (Fig. 4A). In the pituitary gland, gonadotropin-related genes were broadly downregulated, including gonadotropin α-subunit (*gthα*), follicle-stimulating hormone β-subunit (*fshβ*), and luteinizing hormone β-subunit (*lhβ*) (Fig. 4B). Expression of five gonadotropin-releasing hormone receptors was also significantly decreased, including *gnrhr*, *gnrhr1α*, *gnrhr1β*, *gnrhr2*, and *gnrhr4* (Fig. 4B). In the gonads, key steroidogenic enzymes genes such as *cyp11a1*, *cyp17a1*, and *cyp19a1a* were significantly downregulated (Fig. 4C). In addition, several hormone receptors and steroidogenesis-related regulators, including *lhr*, *fshr*, *3β-hsd*, *star*, and *ddit4*, were also downregulated (Fig. 4C). Conversely, Krüppel-like factor 9 (*klf9*) was significantly upregulated (Fig. 4C). Additionally, insulin-like growth factor 3 (*igf3*) expression remained unchanged (Fig. 4C).

3.5. Effects of RU486 on DXMS-induced changes in key HPG axis genes

In *in vitro* cultured brain cells, DXMS significantly downregulated the expression of *cgnrh* and *cox2* (Fig. 5A), while the expression of *mghrh* and *tac3* remained unchanged (Fig. 5A). RU486 pretreatment reversed *cox2* downregulation and partially restored *cgnrh* and *kisspeptin1* expression to levels not significantly different from the control (Fig. 5A). In cultured pituitary cells, DXMS significantly suppressed the expression of *gthα*, *fshβ*, and *gnrhr2* (Fig. 5B), whereas other gonadotropin-related genes, including *lhβ*, *gnrhr*, *gnrhr1α*, *gnrhr1β*, and *gnrhr4*, were unaffected (Fig. 5B). In gonadal cultures, DXMS markedly downregulated key steroidogenic enzymes genes (*cyp11a1*, *cyp17a1*, *3β-hsd*) (Fig. 5C), the receptor *fshr*, and early ovarian development genes (*bmp15*, *gdf9*), while RU486 pretreatment significantly reversed these effects (Fig. 5C). Although *cyp19a1a* was slightly reduced, RU486 restored its expression (Fig. 5C). *Star*, *lhr*, *inhba*, and *inhbb* remained unchanged (Fig. 5C). Additionally, *ddit4* and *klf9*, genes related to stress and development, were upregulated by DXMS and reversed by RU486 (Fig. 5C), while *igf3* was suppressed and also recovered with RU486 (Fig. 5C).

4. Discussion

Stress-induced inhibition of the reproductive system has been widely studied, with GCs, steroid hormones mainly produced by the interrenal tissue (analogous to the adrenal cortex in mammals), responding to stress via binding to the GR. In this study, we successfully cloned and characterized the two *gr* genes (*gr1* and *gr2*) in the Japanese eel. Phylogenetic analysis revealed that the two GR sequences consistently clustered into the classical GR1 and GR2 branches within teleost fish. This phylogenetic pattern is consistent with the classical pattern in which two copies of GRs are retained after the T-WGD, with both *gr1* and *gr2* being preserved over time in most teleosts following genome duplication and divergence (Bury et al., 2003).

In most teleost fish, *gr1* and *gr2* typically exhibit tissue-specific expression patterns. For example, in black rockfish (*Sebastes schlegelii*),

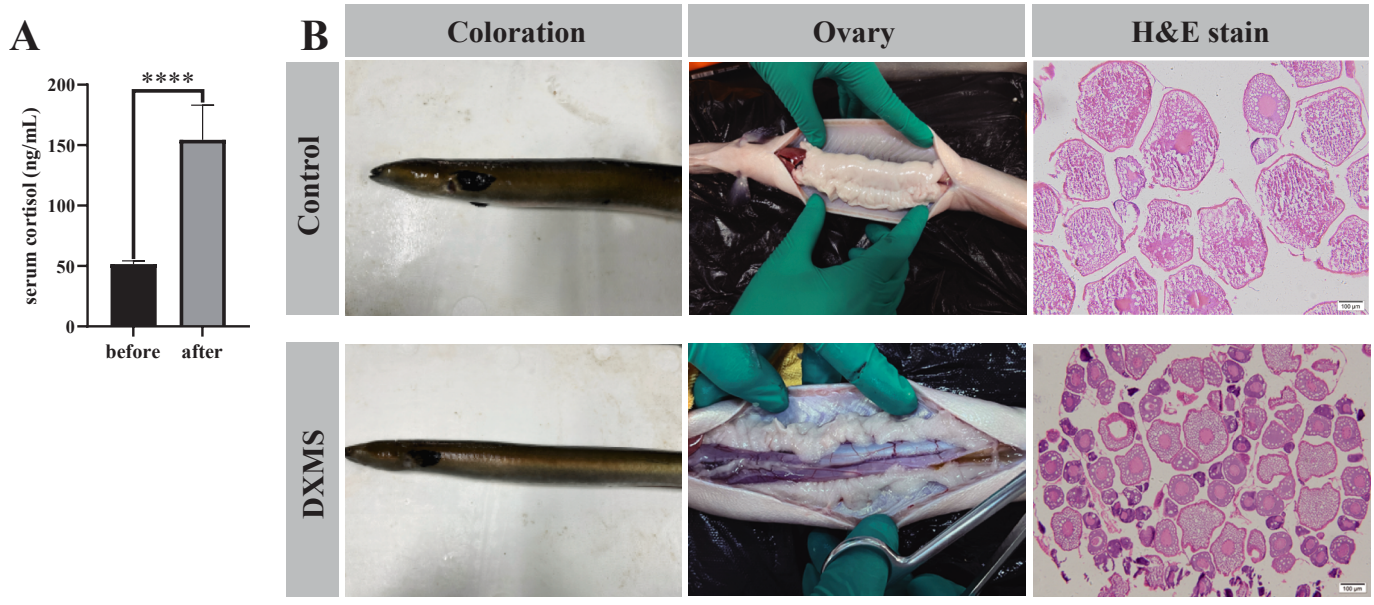

Fig. 3. Serum cortisol levels (A) before and after injection, and ovarian morphology in the DXMS-treated and maturation-induced groups (B). A. Serum cortisol levels (****$P < 0.0001$); B. Ovarian gross morphology and H&E-stained sections in the DXMS-treated vs. maturation-induced groups.

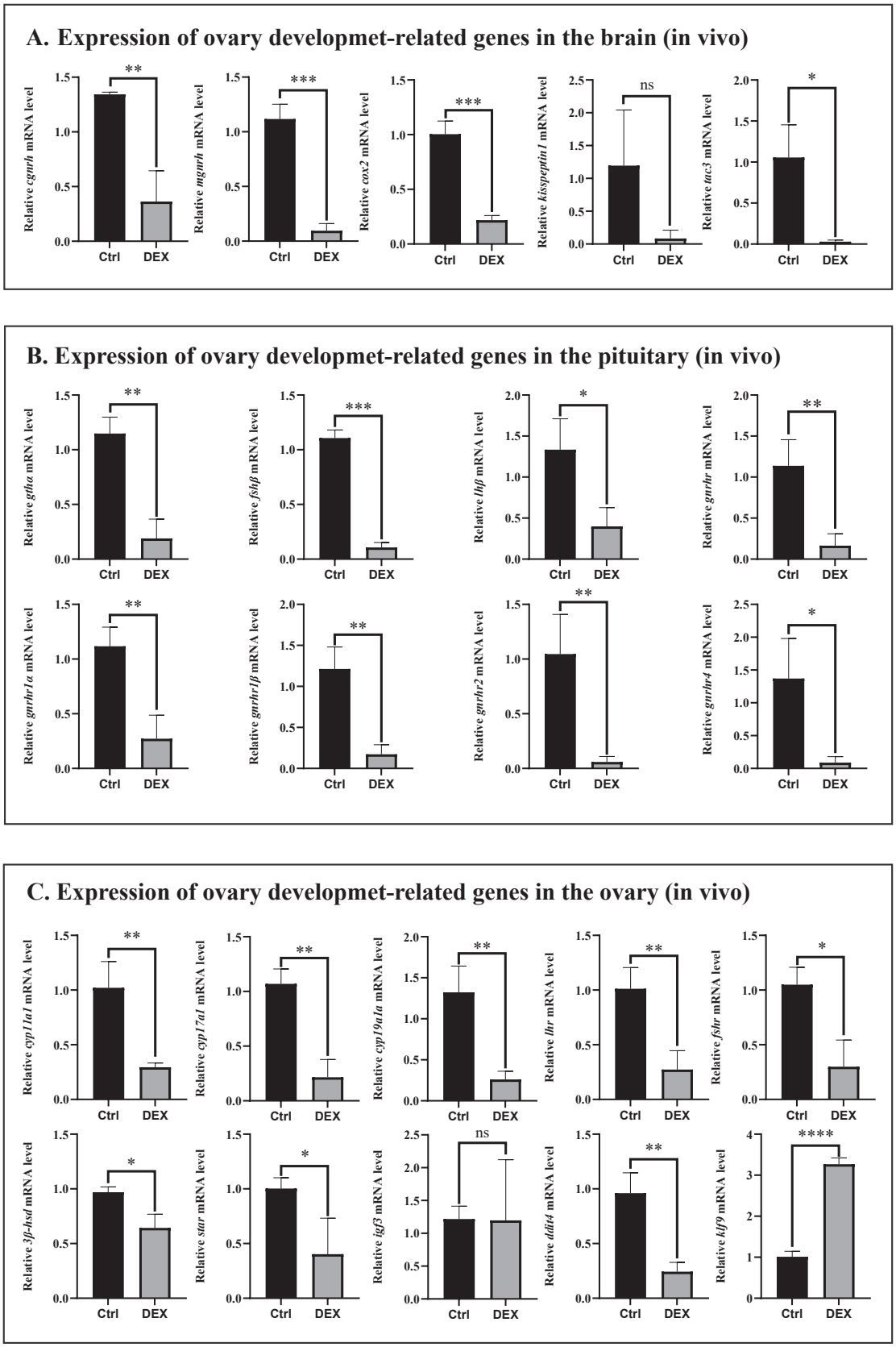

Fig. 4. Effects of DXMS injections on the gene expression of brain, pituitary and ovarian tissues. A: Relative mRNA levels of *cgnrh*, *mgnrh*, *cox2*, *kisspeptin1*, *tac3* (*$P <$ 0.05, **$P < 0.01$, ***$P < 0.001$). B: Relative mRNA levels of *gthα*, *fshβ*, *lhβ*, *gnrhr*, *gnrhr1α*, *gnrhr1β*, *gnrhr2*, *gnrhr4* (*$P < 0.05$, **$P < 0.01$, ***$P < 0.001$). C: Relative mRNA levels of *cyp11a1*, *cyp17a1*, *cyp19a1a*, *lhr*, *fshr*, *3β-hsd*, *star*, *igf3*, *ddit4*, *klf9* (*$P < 0.05$, **$P < 0.01$, ***$P < 0.001$, ****$P < 0.0001$).

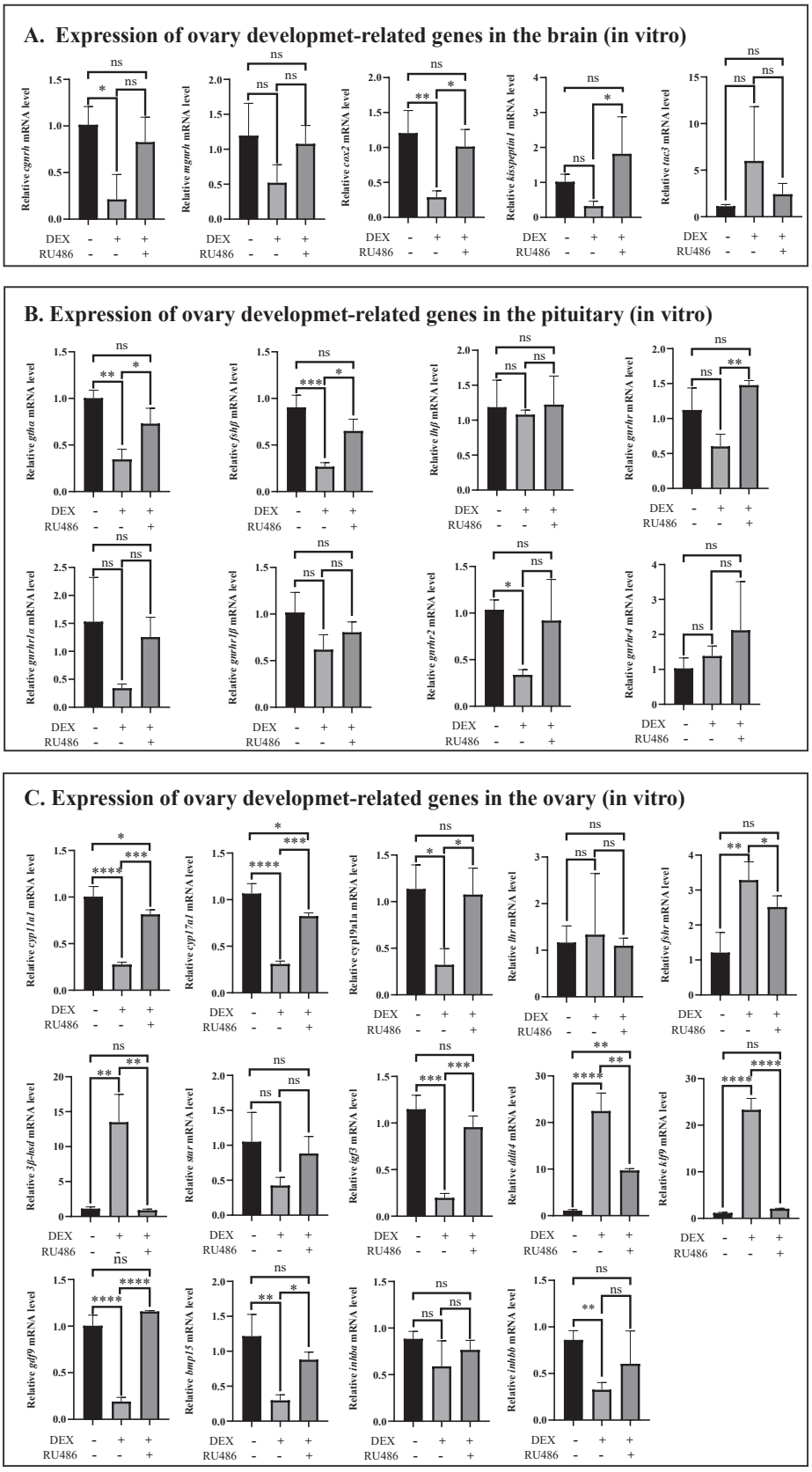

Fig. 5. Effects of DXMS and RU486 stimulation on the gene expression of brain, pituitary and ovarian cells. A: Relative mRNA levels of *cgnrh*, *mgnrh*, *cox2*, *kiss-peptin1*, *tac3* (*$P < 0.05$, **$P < 0.01$). B: Relative mRNA levels of *gthα*, *fshβ*, *lhβ*, *gnrhr*, *gnrhr1α*, *gnrhr1β*, *gnrhr2*, *gnrhr4* (*$P < 0.05$, **$P < 0.01$). C: Relative mRNA levels of *cyp11a1*, *cyp17a1*, *cyp19a1a*, *lhr*, *fshr*, *3β-hsd*, *star*, *igf3*, *ddit4*, *klf9*, *gdf9*, *bmp15*, *inhba*, *inhbb* (*$P < 0.05$, **$P < 0.01$, ***$P < 0.001$, ****$P < 0.0001$).

gr1 and *gr2* were highly expressed in the spleen and kidney (Wang et al., 2022), while in yellow croaker (*Larimichthys crocea*), their expression was high in the heart and brain (He et al., 2022). In the Japanese eel, both genes were highly expressed in the ovary and brain, with moderate levels in the pituitary, covering the main components of the HPG axis. ISH confirmed their localization to oocytes in the ovary, hypothalamic nuclei (NPO and NPP) closely associated with GnRH neurons (Amano et al., 2014), and pituitary regions (RPD, PPD, NH). This coordinated distribution suggests that GRs integrate HPI and HPG axis regulation, allowing cortisol to influence both stress responses and reproductive endocrine functions, potentially via modulation of GnRH rhythms (López-Olmeda et al., 2013).

The Japanese eel is a "stress-tolerant, dark-preferring" species (Amano et al., 2021). Under acute stress, serum cortisol can increase tenfold (Bern and Madsen, 1992; Bonga, 1997). In this study, repeated handling and hormonal stimulation during artificial reproduction maintained chronic HPI activation, as shown by elevated serum cortisol in saline-injected eels. Separately, long-term DXMS treatment impaired ovarian development at a non-lethal dose, as evidenced by gross morphology and histological sections. After 12 weeks, *in vivo* DXMS administration significantly suppressed the expression of key HPG genes, indicating a systemic inhibitory effect of GR signaling on reproduction. Similar effects of prolonged cortisol exposure have been observed in *Sparus aurata* and *Micropterus dolomieu* (Algera et al., 2017; Jerez-Cepa et al., 2019).

The HPG axis regulates ovarian function through dynamic interactions among central, pituitary, and gonadal hormonal signals, involving multiple key genes associated with follicular development, steroidogenesis, and sex steroid feedback regulation (Fanis et al., 2023). In the brain, DXMS downregulated *cgnrh* and *mgnrh*, consistent with chronic stress disrupting GnRH rhythms (Ciechanowska et al., 2016). The downregulation of *cox2* and *tac3* suggests that GC may inhibit neuropeptide and pro-inflammatory pathways, thereby interfering with GnRH neuron activation and pulsatile release (Hu et al., 2014). However, *kisspeptin1* expression remained unchanged, possibly due to its stage-specific regulatory complexity in the Japanese eel (Anderson, 2024). At the pituitary level, *gnrhr*, *gthα*, *fshβ* and *lhβ* were suppressed, though *lhβ* inhibition was weaker than *fshβ*, in line with mammalian findings of differential GC effects on gonadotropins (Padmanabhan et al., 1983; Li and Wagner, 1983). At the gonadal level, DXMS markedly downregulated the steroidogenic enzymes genes *cyp11a1*, *cyp17a1*, and *cyp19a1a*, impairing sex steroid synthesis (Zhu et al., 2021), while reduced expression of *lhr*, *fshr*, *3β-hsd*, *star*, and *ddit4* further indicated disruption of gonadal endocrine regulation. The upregulation of *klf9* confirmed GR pathway activation (Gans et al., 2020; Liu et al., 2016). Conversely, stable *igf3* expression suggests that some pro-reproductive signals are preserved under homeostatic control despite chronic stress.

Taken together, these data demonstrate clear interactions among GCs, GnRH, gonadotropins, kisspeptin, steroid hormones, and growth factors, highlighting that stress-induced GR signaling disrupts multiple interconnected levels of reproductive regulation rather than isolated pathways.

GCs exert inhibitory effects across all levels of the HPG axis, and our *in vitro* assays confirmed that these effects are mediated by GR. Treatment of brain, pituitary, and ovarian cells with DXMS suppressed key reproductive genes, while co-treatment with RU486 effectively reversed most of these changes, providing direct evidence for GR-dependent regulation (Breen and Karsch, 2006).

Specifically, In the brain, *in vitro* DXMS treatment significantly downregulated *cgnrh* expression, an effect reversed by RU486, consistent with GR-mediated inhibition of GnRH signaling and previous findings in zebrafish (Khor et al., 2016). *Kisspeptin1* and *cox2* were also suppressed and reversed, confirming GR-mediated inhibition of inflammatory and neuropeptide pathways (Chivers et al., 2004; Khor et al., 2016; Park et al., 2023), though *mgnrh* and *tac3* were less responsive.

At the pituitary level, DXMS treatment significantly decreased the expression of *gthα*, *fshβ* and *gnrhr*, partially restored by RU486, consistent with GR-mediated suppression of gonadotropin synthesis and GnRH responsiveness (Fernandes, 2006). Notably, *lhβ* was less affected, suggesting differential GR sensitivity among gonadotropin subunits.

In ovarian cells, DXMS suppressed key steroidogenic enzymes genes (*cyp11a1*, *cyp17a1*, *cyp19a1a*) and several growth factors (*igf3*, *bmp15*, *gdf9*), all reversed by RU486. These results indicate that GR activation not only disrupts estrogen synthesis but also impairs local paracrine signals essential for follicular development (Hajime et al., 1988; Peng et al., 2013). Upregulation of classical GR targets (*ddit4*, *klf9*) confirmed transcriptional activation via GR (Hoffman et al., 2022; Wong et al., 2010). Interestingly, DXMS upregulated *fshr* and *3β-hsd*, reversed by RU486, suggesting complex GR effects on receptor and metabolic gene expression (Asser et al., 2014).

5. Conclusion

In summary, this study cloned and characterized the two *gr* genes (*gr1* and *gr2*) in the Japanese eel, confirming their evolutionary conservation and high expression in reproductive tissues. Functional assays demonstrated that GR activation by DXMS suppresses genes involved in GnRH signaling, gonadotropin synthesis, steroidogenesis, and local growth factor pathways, while RU486 reversed most of these effects, highlighting the specificity of GR-mediated regulation. These findings provide mechanistic evidence that GCs disrupt reproduction not only by inhibiting the HPG axis broadly, but through coordinated interference with GnRH, Gth, kisspeptin, steroid hormones, and ovarian growth factors. This integrative perspective advances our understanding of stress-reproduction interactions in eels and offers a foundation for improving artificial breeding strategies.

CRediT authorship contribution statement

Xuanhan Zhang: Writing – original draft, Data curation. **Chenpeng Zuo:** Investigation, Data curation. **Jiaqi Liu:** Data curation. **Xiao Jing:** Data curation. **Ziyi Zhao:** Data curation. **Jing Yang:** Data curation. **Zhijun Wang:** Resources. **Xin Qi:** Writing – review & editing, Methodology, Funding acquisition, Conceptualization.

Declaration of competing interest

The authors declare that they have no known competing financial interests or personal relationships that could have appeared to influence the work reported in this paper.

Acknowledgments

This research was supported by **The** National Natural Science Foundation of China **with grant number [**32270556**]**.

Data availability

Data will be made available on request.

References

Algera, D.A., Gutowsky, L.F.G., Zolderdo, A.J., Cooke, S.J., 2017. Parental care in a Algera, D.A., Gutowsky, L.F.G., Zolderdo, A.J., Cooke, S.J., 2017. Parental care in a stressful world: Experimentally elevated cortisol and brood size manipulation influence nest success probability and nest-tending behavior in a wild teleost fish. Physiol. Biochem. Zool. 90, 318–329. https://doi.org/10.1086/689678.

Amano, M., Amiya, N., Mizusawa, K., Chiba, H., 2021. Effects of background color and rearing density on stress-related hormones in the juvenile Japanese eel *Anguilla japonica*. Fish. Sci. 87, 521–528. https://doi.org/10.1007/s12562-021-01527-4.

Amano, M., Mizusawa, N., Okubo, K., Amiya, N., Mizusawa, K., Chiba, H., Yamamoto, N., Takahashi, A., 2014. Cloning of corticotropin-releasing hormone (CRH) precursor cDNA and immunohistochemical detection of CRH peptide in the

brain of the Japanese eel, paying special attention to gonadotropin-releasing hormone. Cell Tissue Res. 356, 243–251. https://doi.org/10.1007/s00441-013-1784-6.
Anderson, R.A., 2024. Kisspeptin and neurokinin B neuroendocrine pathways in the control of human ovulation. J. Neuroendocrinol. 36, e13371. https://doi.org/10.1111/jne.13371.
Arterbery, A.S., Fergus, D.J., Fogarty, E.A., Mayberry, J., Deitcher, D.L., Lee Kraus, W., Bass, A.H., 2011. Evolution of ligand specificity in vertebrate corticosteroid receptors. BMC Evol. Biol. 11, 14. https://doi.org/10.1186/1471-2148-11-14.
Asser, L., Hescot, S., Viengchareun, S., Delemer, B., Trabado, S., Lombès, M., 2014. Autocrine positive regulatory feedback of glucocorticoid secretion: glucocorticoid receptor directly impacts H295R human adrenocortical cell function. Mol. Cell. Endocrinol. 395, 1–9. https://doi.org/10.1016/j.mce.2014.07.012.
Bern, H.A., Madsen, S.S., 1992. A selective survey of the endocrine system of the rainbow trout (*Oncorhynchus mykiss*) with emphasis on the hormonal regulation of ion balance. Aquaculture 100, 237–262. https://doi.org/10.1016/0044-8486(92)90384-W.
Blanes-García, M., García-Salinas, P., Morini, M., Pérez, L., Asturiano, J.F., Gallego, V., 2022. Using osmotic pumps to induce the production of gametes in male and female European eels. Animals 12, 387. https://doi.org/10.3390/ani12030387.
Bonga, S.E.W., 1997. The stress response in fish. Physiol. Rev. https://doi.org/10.1152/physrev.1997.77.3.591.
Bourke, C.H., Harrell, C.S., Neigh, G.N., 2012. Stress-induced sex differences: Adaptations mediated by the glucocorticoid receptor. Hormones and Behavior, Special Issue: the Neuroendocrine-Immune Axis in Health and Disease 62, 210–218. https://doi.org/10.1016/j.yhbeh.2012.02.024.
Breen, K., Karsch, F., 2006. New insights regarding glucocorticoids, stress and gonadotropin suppression. Front. Neuroendocrinol. 27, 233–245. https://doi.org/10.1016/j.yfrne.2006.03.335.
Bury, N.R., 2017. The evolution, structure and function of the ray finned fish (*Actinopterygii*) glucocorticoid receptors. General and Comparative Endocrinology, Special Issue on International Symposium on Comparative Endocrinology and Integrative Physiology - CEIP 2015 (251), 4–11. https://doi.org/10.1016/j.ygcen.2016.06.030.
Bury, N.R., Sturm, A., Rouzic, P.L., Lethimonier, C., Ducouret, B., Guiguen, Y., Robinson-Rechavi, M., Laudet, V., Rafestin-Oblin, M.E., Prunet, P., 2003. Evidence for two distinct functional glucocorticoid receptors in teleost fish. Mol. Endocrinol. 31, 141–156. https://doi.org/10.1677/jme.0.0310141.
Charmandari, E., Tsigos, C., Chrousos, G., 2005. Endocrinology of the stress Response1. Annu. Rev. Physiol. 67, 259–284. https://doi.org/10.1146/annurev.physiol.67.040403.120816.
Chivers, J.E., Cambridge, L.M., Catley, M.C., Mak, J.C., Donnelly, L.E., Barnes, P.J., Newton, R., 2004. Differential effects of RU486 reveal distinct mechanisms for glucocorticoid repression of prostaglandin E2 release. Eur. J. Biochem. 271, 4042–4052. https://doi.org/10.1111/j.1432-1033.2004.04342.x.
Ciechanowska, M., Łapot, M., Antkowiak, B., Mateusiak, K., Paruszewska, E., Malewski, T., Paluch, M., Przekop, F., 2016. Effect of short-term and prolonged stress on the biosynthesis of gonadotropin-releasing hormone (GnRH) and GnRH receptor (GnRHR) in the hypothalamus and GnRHR in the pituitary of ewes during various physiological states. Anim. Reprod. Sci. 174, 65–72. https://doi.org/10.1016/j.anireprosci.2016.09.006.
Dinarello, A., Licciardello, G., Fontana, C.M., Tiso, N., Argenton, F., Valle, L.D., 2020. Glucocorticoid receptor activities in the zebrafish model: a review. J. Endocrinol. 246, R13–R31. https://doi.org/10.1530/JOE-20-0173.
Fanis, P., Neocleous, V., Papapetrou, I., Phylactou, L.A., Skordis, N., 2023. Gonadotropin-releasing hormone receptor (GnRHR) and hypogonadotropic hypogonadism. Int. J. Mol. Sci. 24, 15965. https://doi.org/10.3390/ijms242115965.
Fernandes, S.M., 2006. Transcriptional regulation of the Gonadotropin-Releasing Hormone Receptor (GnRHR) gene by Glucocorticoids. MSc Thesis, University of Stellenbosch, South Africa. Available at: https://core.ac.uk/display/37347178.
Fernandino, J.I., Hattori, R.S., Kishii, A., Strüssmann, C.A., Somoza, G.M., 2012. The Cortisol and Androgen Pathways Cross talk in High Temperature-Induced Masculinization: the 11β-Hydroxysteroid Dehydrogenase as a Key Enzyme. Endocrinology 153, 6003–6011. https://doi.org/10.1210/en.2012-1517.
Gans, I., Hartig, E.I., Zhu, S., Tilden, A.R., Hutchins, L.N., Maki, N.J., Graber, J.H., Coffman, J.A., 2020. Klf9 is a key feedforward regulator of the transcriptomic response to glucocorticoid receptor activity. Sci. Rep. 10, 11415. https://doi.org/10.1038/s41598-020-68040-z.
Gopurappilly, R., Ogawa, S., Parhar, I., 2012. Functional significance of GnRH and kisspeptin, and their cognate receptors in teleost reproduction. Front. Endocrinol. 4, 24. https://doi.org/10.3389/fendo.2013.00024.
Hajime, N., Kishio, O., Masao, O., Ken-Ichi, K., Hiroshi, I., 1988. RU486 inhibits induction of aromatase by dexamethasone via glucocorticoid receptor in cultured human skin fibroblasts. J. Steroid Biochem. 29, 63–68. https://doi.org/10.1016/0022-4731(88)90377-9.
He, L., Shi, X., Zeng, X., Zhou, F., Lan, T., Chen, M., Han, K., 2022. Characterization of the glucocorticoid receptor of large yellow croaker (*Larimichthys crocea*) and its expression in response to salinity and immune stressors. Comp. Biochem. Physiol. A Mol. Integr. Physiol. 265, 111124. https://doi.org/10.1016/j.cbpa.2021.111124.
Hoffman, J.A., Trotter, K.W., Day, C.R., Ward, J.M., Inoue, K., Rodriguez, J., Archer, T. K., 2022. Multimodal regulatory elements within a hormone-specific super enhancer control a heterogeneous transcriptional response. Mol. Cell 82, 803–815.e5. https://doi.org/10.1016/j.molcel.2021.12.035.
Hu, G., Lin, C., He, M., Wong, A.O.L., 2014. Neurokinin B and reproductive functions: "KNDy neuron" model in mammals and the emerging story in fish. Gen. Comp. Endocrinol. 208, 94–108. https://doi.org/10.1016/j.ygcen.2014.08.009.
Jerez-Cepa, I., Gorissen, M., Mancera, J.M., Ruiz-Jarabo, I., 2019. What can we learn from glucocorticoid administration in fish? Effects of cortisol and dexamethasone on intermediary metabolism of gilthead seabream (*Sparus aurata* L.). Comp. Biochem. Physiol. A Mol. Integr. Physiol. 231, 1–10. https://doi.org/10.1016/j.cbpa.2019.01.010.
Jiang, J., Young, G., Kobayashi, T., Nagahama, Y., 1998. Eel (*Anguilla japonica*) testis 11β-hydroxylase gene is expressed in interrenal tissue and its product lacks aldosterone synthesizing activity. Mol. Cell. Endocrinol. 146, 207–211. https://doi.org/10.1016/S0303-7207(98)00147-6.
Kagawa, H., Iinuma, N., Tanaka, H., Ohta, H., Okuzawa, K., 1998. Effects of rearing period in seawater on induced maturation in female Japanese eel *Anguilla japonica*. Fish. Sci. 64, 77–82. https://doi.org/10.2331/fishsci.64.77.
Kazeto, Y., Kohara, M., Tosaka, R., Gen, K., Yokoyama, M., Miura, C., Miura, T., Adachi, S., Yamauchi, K., 2012. Molecular Characterization and Gene Expression of Japanese Eel (anguilla Japonica) Gonadotropin Receptors. jzoo 29, 204–211. https://doi.org/10.2108/zsj.29.204.
Khor, Y.M., Soga, T., Parhar, I.S., 2016. Early-life stress changes expression of GnRH and kisspeptin genes and DNA methylation of GnRH3 promoter in the adult zebrafish brain. Gen. Comp. Endocrinol. 227, 84–93. https://doi.org/10.1016/j.ygcen.2015.12.004.
Kirby, E.D., Geraghty, A.C., Ubuka, T., Bentley, G.E., Kaufer, D., 2009. Stress increases putative gonadotropin inhibitory hormone and decreases luteinizing hormone in male rats. PNAS 106, 11324–11329. https://doi.org/10.1073/pnas.0901176106.
Knight, P.G., Glister, C., 2006. TGF-β Superfamily Members and Ovarian Follicle Development. https://doi.org/10.1530/rep.1.01074.
Kumar, R., Thompson, E.B., 2005. Gene regulation by the glucocorticoid receptor: Structure: function relationship. J. Steroid Biochem. Mol. Biol. 94, 383–394. https://doi.org/10.1016/j.jsbmb.2004.12.046.
Lai, X.J., Peng, S., Wang, Y.L., 2022. Dynamic transcriptome analysis of ovarian follicles in artificial maturing Japanese eel (*Anguilla japonica*). Theriogenology 180, 176–188. https://doi.org/10.1016/j.theriogenology.2021.12.031.
Lee, M.-S., Choi, H.-S., Kwon, S.-H., Morita, K., Her, S., 2009. Identification of the functional domain of glucocorticoid receptor involved in RU486 antagonism. J. Steroid Biochem. Mol. Biol. 117, 67–73. https://doi.org/10.1016/j.jsbmb.2009.07.005.
Li, P.S., Wagner, W.C., 1983. In vivo and in vitro studies on the effect of adrenocorticotropic hormone or cortisol on the pituitary response to gonadotropin-releasing hormone. Biol. Reprod. 29, 25–37. https://doi.org/10.1095/biolreprod29.1.25.
Li, Y., Sturm, A., Cunningham, P., Bury, N.R., 2012. Evidence for a divergence in function between two glucocorticoid receptors from a basal teleost. BMC Evol. Biol. 12, 137. https://doi.org/10.1186/1471-2148-12-137.
Liu, X., Wang, Y., Ortlund, E.A., 2019. First high-resolution crystal structures of the glucocorticoid receptor ligand-binding domain–peroxisome proliferator-activated γ coactivator 1-α complex with endogenous and synthetic glucocorticoids. Mol. Pharmacol. 96, 408–417. https://doi.org/10.1124/mol.119.116806.
Liu, X.-H., Xie, B.-W., Wang, Z.-J., Jin, L., Zhang, Y.-G., 2016. The secretion, synthesis, and metabolism of cortisol and its downstream genes in the H–P–I axis of rare minnows (*Gobiocypris rarus*) are disrupted by acute waterborne cadmium exposure. Comp. Biochem. Physiol. C: Toxicol. Pharmacol. 185–186, 112–121. https://doi.org/10.1016/j.cbpc.2016.03.009.
López-Olmeda, J.F., Blanco-Vives, B., Pujante, I.M., Wunderink, Y.S., Mancera, J.M., Sánchez-Vázquez, F.J., 2013. Daily rhythms in the hypothalamus-pituitary-interrenal axis and acute stress responses in a teleost flatfish, *Solea senegalensis*. Chronobiol. Int. 30, 548–561. https://doi.org/10.3109/07420528.2012.754448.
Lutton, B.V., Callard, I.P., 2008. Influence of reproductive activity, sex steroids, and seasonality on epigonal organ cellular proliferation in the skate (*Leucoraja erinacea*). Gen. Comp. Endocrinol. 155, 116–125. https://doi.org/10.1016/j.ygcen.2007.03.011.
Milla, S., Wang, N., Mandiki, S.N.M., Kestemont, P., 2009. Corticosteroids: Friends or foes of teleost fish reproduction? Comp. Biochem. Physiol. A Mol. Integr. Physiol. 153, 242–251. https://doi.org/10.1016/j.cbpa.2009.02.027.
Mukuda, T., Ando, M., 2003. Brain atlas of the Japanese eel: Comparison to other fishes. Mem. Fac. Integr. Arts Sci., Hiroshima Univ., Ser. IV. Sci. Rep. 29, 1–25. https://doi.org/10.15027/159.
Murugananthkumar, R., Sudhakumari, C.-C., 2022. Understanding the impact of stress on teleostean reproduction. Aquacult. Fish. 7, 553–561. https://doi.org/10.1016/j.aaf.2022.05.001.
Padmanabhan, V., Keech, C., Convey, E.M., 1983. Cortisol inhibits and adrenocorticotropin has no effect on luteinizing hormone-releasing hormone-induced release of luteinizing hormone from bovine pituitary cells in vitro. Endocrinology 112, 1782–1787. https://doi.org/10.1210/endo-112-5-1782.
Park, Y.-J., Heo, J., Kim, Y., Cho, H., Shim, M., Im, K., Lim, W., 2023. Glucocorticoids alleviate particulate matter-induced COX-2 expression and mitochondrial dysfunction through the bcl-2/GR complex in A549 cells. Sci. Rep. 13, 18884. https://doi.org/10.1038/s41598-023-46257-y.
Peng, J., Li, Q., Wigglesworth, K., Rangarajan, A., Kattamuri, C., Peterson, R.T., Eppig, J. J., Thompson, T.B., Matzuk, M.M., 2013. Growth differentiation factor 9:Bone morphogenetic protein 15 heterodimers are potent regulators of ovarian functions. Proc. Natl. Acad. Sci. U.S.A. 110. https://doi.org/10.1073/pnas.1218020110.
Pierce, A.L., Dickey, J.T., Felli, L., Swanson, P., Dickhoff, W.W., 2010. Metabolic hormones regulate basal and growth hormone-dependent *igf2* mRNA level in primary cultured coho salmon hepatocytes: Effects of insulin, glucagon, dexamethasone, and triiodothyronine. J. Endocrinol. 205, 37–47. https://doi.org/10.1677/JOE-09-0338.

Reinecke, M., 2010. Insulin-like growth factors and fish reproduction. Biol. Reprod. 82, 656–661. https://doi.org/10.1095/biolreprod.109.080093.

Reyes-López, F.E., Aerts, J., Vallejos-Vidal, E., Ampe, B., Dierckens, K., Tort, L., Bossier, P., 2018. Modulation of innate immune-related genes and glucocorticoid synthesis in gnotobiotic full-sibling european sea bass (*Dicentrarchus labrax*) larvae challenged with Vibrio anguillarum. Front. Immunol. 9, 914. https://doi.org/10.3389/fimmu.2018.00914.

Somoza, G.M., Mechaly, A.S., Trudeau, V.L., 2020. Kisspeptin and GnRH interactions in the reproductive brain of teleosts. Gen. Comp. Endocrinol. 298, 113568. https://doi.org/10.1016/j.ygcen.2020.113568.

Suarez-Bregua, P., Guerreiro, P.M., Rotllant, J., 2018. Stress, glucocorticoids and bone: a review from mammals and fish. Front. Endocrinol. 9. https://doi.org/10.3389/fendo.2018.00526.

Tokuda, Y., Touhata, K., Kinoshita, M., Toyohara, H., Sakaguchi, M., Yokoyama, Y., Ichikawa, T., Yamashita, S., 1999. Sequence and expression of a cDNA encoding japanese flounder glucocorticoid receptor. Fish. Sci. 65, 466–471. https://doi.org/10.2331/fishsci.65.466.

Vazzana, M., Vizzini, A., Sanfratello, M.A., Celi, M., Salerno, G., Parrinello, N., 2010. Differential expression of two glucocorticoid receptors in seabass (*Dicentrarchus labrax*) head kidney after exogeneous cortisol inoculation. Comp. Biochem. Physiol. A Mol. Integr. Physiol. 157, 49–54. https://doi.org/10.1016/j.cbpa.2010.05.003.

Wang, X., Meng, W., Qi, X., Li, Y., Li, J., Lyu, L., Li, J., Yao, Y., Yan, S., Zuo, C., Xie, S., Wen, H., 2022. Molecular characterization and expression patterns of glucocorticoid receptors in the viviparous black rockfish *Sebastes schlegelii*. Gen. Comp. Endocrinol. 316, 113947. https://doi.org/10.1016/j.ygcen.2021.113947.

Weikum, E.R., Liu, X., Ortlund, E.A., 2018. The nuclear receptor superfamily: a structural perspective. Protein Sci. 27, 1876–1892. https://doi.org/10.1002/pro.3496.

Weltzien, F.-A., Andersson, E., Andersen, Ø., Shalchian-Tabrizi, K., Norberg, B., 2004. The brain–pituitary–gonad axis in male teleosts, with special emphasis on flatfish (*Pleuronectiformes*). Comp. Biochem. Physiol. A Mol. Integr. Physiol. 137, 447–477. https://doi.org/10.1016/j.cbpb.2003.11.007.

Whirledge, S., Cidlowski, J.A., 2013. A role for glucocorticoids in stress-impaired reproduction: beyond the hypothalamus and pituitary. Endocrinology 154, 4450–4468. https://doi.org/10.1210/en.2013-1652.

Wong, S., Tan, K., Carey, K.T., Fukushima, A., Tiganis, T., Cole, T.J., 2010. Glucocorticoids stimulate hepatic and renal catecholamine inactivation by direct rapid induction of the dopamine sulfotransferase Sult1d1. Endocrinology 151, 185–194. https://doi.org/10.1210/en.2009-0590.

Zhu, L., Liu, Y., Xue, X., Yuan, C., Wang, Z., 2021. BPA's transgenerational disturbance to transcription of ovarian steroidogenic genes in rare minnow gobiocypris rarus via DNA and histone methylation. Sci. Total Environ. 762, 143055. https://doi.org/10.1016/j.scitotenv.2020.143055.

Zmora, N., Stubblefield, J., Zulperi, Z., Biran, J., Levavi-Sivan, B., Muñoz-Cueto, J.A., Zohar, Y., 2012. Differential and gonad stage-dependent roles of Kisspeptin1 and Kisspeptin2 in reproduction in the modern teleosts. Morone Species1. https://doi.org/10.1095/biolreprod.111.097667.